

Spectrum and composition of galactic cosmic rays accelerated in supernova remnants

Vladimir Ptuskin*, Eun-Suk Seo†, Vladimir Zirakashvili*

*IZMIRAN, Troitsk, Moscow region 142190, Russia

†IPST, University of Maryland, College Park, MD 29742 USA

Abstract. The spectra of high-energy protons and nuclei accelerated by supernova remnant shocks are calculated taking into account magnetic field amplification and Alfvénic drift for different types of SNRs during their evolution. The overall energy spectrum and elemental composition of cosmic rays after propagation through the Galaxy are found.

Keywords: acceleration, spectrum, SNR, shocks

I. INTRODUCTION

The supernova remnants (SNRs) are recognized as the principle sources of Galactic cosmic rays, and the diffusive shock acceleration is accepted as the acceleration mechanism of cosmic rays by a supernova blast wave moving through the turbulent interstellar medium. Accelerated by supernova shocks, the energetic particles diffuse in the interstellar magnetic fields and fill the entire Galaxy. Clear evidence for particle acceleration in SNRs is given by observations of non-thermal radio, X-ray, and gamma-ray radiation. It is experimentally established from the H.E.S.S. data that there are cosmic-ray particles with energies exceeding 10^{14} eV in the shell of the supernova remnant RX J1713.7-3946 [1].

For a time, the theoretical estimates of maximum proton energy were at a level of $E_{\max} \approx 10^{14} - 10^{15}$ eV [2]. The work [3] demonstrated that a very large random magnetic field $\delta B \gg B_{\text{ism}}$ (where $B_{\text{ism}} \approx 5 \mu\text{G}$ is the average interstellar field upstream of the shock) can be generated by cosmic-ray streaming instability in the precursor of strong shocks. It results then in efficient confinement of energetic particles in the shock vicinity, and it may rise the maximum particle energy by about two orders of magnitude (the exact value depends on the supernova parameters, see below). Remarkably, data on synchrotron X-ray emission from a number of young SNRs proved the presence of strong magnetic fields 150 to 500 μG [4] that can be naturally explained by the effect of cosmic-ray streaming instability.

In the present work we calculate the steady state spectrum of cosmic rays in the Galaxy using recent results on magnetic field amplification in SNRs.

II. CALCULATION OF COSMIC RAY SPECTRUM IN THE GALAXY

Because of high efficiency of shock acceleration, the spectrum of cosmic rays should be selfconsistently determined with the account of shock modification caused

by the pressure of accelerated particles. We study cosmic ray acceleration and the evolution of a supernova blast wave with the use of our numerical code described in [5] (see also the paper "Numerical simulations of shock acceleration in SNRs including magnetic field amplification" by Zirakashvili and Ptuskin at this Conference for the improved version of the code). The hydrodynamic equations are solved together with the diffusion-convection transport equation for the cosmic ray distribution function $f(t, r, p)$, which depends on time t , radial distance from the point of supernova explosion r (here the spherical symmetry is assumed), and the particle momentum p . The accepted injection efficiency of thermal ions in the process of shock acceleration $\eta = 0.1 u_{\text{sh}}/c$ is taken in accordance with [6]; here $u_{\text{sh}}(t)$ is the varying in time shock velocity and c is the speed of light. The new essential feature of our calculations is the inclusion of the Alfvénic drift effect for particle transport. The Alfvénic velocity $V_A = B/\sqrt{4\pi\rho}$ is not negligible in comparison to the gas velocity u downstream of the shock if the magnetic field is significantly amplified as it follows from the observations of the synchrotron X-ray radiation. The positive (directed outside) gradient of accelerated particles in the downstream region from the shock generates Alfvén waves propagating in the negative direction, and we set the cosmic ray advection velocity equal to $w = u - V_A/\sqrt{3}$ there. Due to this effect, the accelerating particles "feel" a smaller compression ratio and acquire softer energy spectrum compared to the usual assumption $w = u$. We employ results [4] on the analysis of X-ray radiation from young SNRs and assume that magnetic energy density $B^2/8\pi$ downstream of the shock is 3.5 % of the ram pressure ρu_{sh}^2 . It is worth noting that this relation is in a good agreement with the modelling of cosmic ray streaming instability in young SNRs [7].

The Bohm diffusion coefficient $D_B = vpc/(3ZeB)$ is assumed for the accelerating particles of charge Ze and velocity v . The maximum particle momentum p_{\max} reached in a process of diffusive shock acceleration can be roughly estimated from the condition $D_B(p_{\max}) \sim 0.1 u_{\text{sh}} R_{\text{sh}}$ with D_B calculated for the upstream magnetic field, which is about 5 times smaller than the downstream field. This gives an order of magnitude estimate $p_{\max} c/Z \sim 24(u_{\text{sh},3})^2 R_{\text{sh}} \sqrt{n}$ TeV, where $10^3 u_{\text{sh},3}$ km/s is the shock velocity, R_{sh} pc is the shock radius, n cm⁻³ is the interstellar gas number density.

It can be shown, see [8], that the transformation of

supernova explosion energy to cosmic rays becomes efficient from the beginning of the Sedov stage of the shock evolution (i.e. when the mass of supernova ejecta becomes equal to the mass of swept-up gas) and continues later on. As a result, the characteristic knee arises in the overall spectrum of particles accelerated by the evolving supernova remnant. The position of knee p_{knee} can be estimated from the above equations for p_{max} where u_{sh} and R_{sh} are determined at the time when Sedov stage begins. It gives approximately

$$p_{\text{knee}}c/Z \sim 1.1 \cdot 10^{15} E_{51} n^{1/6} M_{\text{ej}}^{-2/3} \text{eV}. \quad (1)$$

Here E_{51} is the kinetic energy of the supernova explosion in units of 10^{51} erg and M_{ej} is the mass of supernova ejecta measured in the solar masses.

If the presupernova had a dense star wind with velocity u_w and the mass loss rate \dot{M} before the explosion, the shock may enter the Sedov stage while propagating through the wind material with mass density $\rho_w = \dot{M}/(4\pi u_w r^2)$. Eq. (1) should be replaced in this case by the following equation:

$$p_{\text{knee}}c/Z \sim 8.4 \cdot 10^{15} E_{51} \sqrt{\dot{M}_{-5}/u_w} M_{\text{ej}}^{-1} \text{eV}. \quad (2)$$

We fulfilled numerical simulations of cosmic ray acceleration for 4 types of supernova remnants.

1. Type Ia SNRs with the following parameters: the kinetic energy of explosion $E = 10^{51}$ erg, the number density of the surrounding interstellar gas $n = 0.1 \text{ cm}^{-3}$, the mass of ejecta $M_{\text{ej}} = 1.4 M_{\odot}$. Also important for accurate calculations is the index k which describes the power law density profile $\rho_s \propto r^{-k}$ of the outer part of the star that freely expands after supernova explosions; $k = 7$ for Type Ia supernova.

2. Type IIP SNRs with parameters $E=10^{51}$ erg, $n = 0.1 \text{ cm}^{-3}$, $M_{\text{ej}} = 8 M_{\odot}$, $k = 12$.

3. Type Ib/c SNRs with $E = 10^{51}$ erg exploding into the low density bubble with density $n = 0.01 \text{ cm}^{-3}$ produced by the progenitor star when it was on the main sequence, $M_{\text{ej}} = 2 M_{\odot}$, $k = 7$.

4. Type IIb SNRs with $E = 3 \cdot 10^{51}$ erg, $n = 0.01 \text{ cm}^{-3}$, $M_{\text{ej}} = 1 M_{\odot}$. Before entering the rarefied bubble, the blast wave goes through the dense wind emitted by the progenitor star during its final RSG (Red Super Giant) stage of evolution. We assume that the mass loss rate by the wind is $\dot{M} = 10^{-4} M_{\odot}/\text{yr}$ and the outer wind radius is 5 pc.

The discussion about properties of SNRs produced by core collapse supernovae can be found in [9].

Based on the statistics of supernovae within 28 Mpc of the Galaxy [10], we accept the following relative rates for the 4 types of supernovae described above: 0.30, 0.44, 0.22, and 0.04 respectively.

The calculated cosmic ray spectra produced over the lifetime of each type of supernovae are shown in Fig.1 under the assumption that only protons are accelerated.

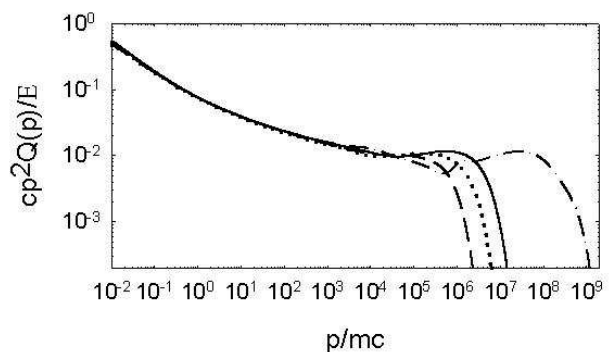


Fig. 1: Proton source spectra produced by supernovae Type Ia (solid line), Type IIP (dash line), Type Ib/c (dotted line), and Type IIb (dash-dot line)

Here $Q(p) = 4\pi p^2 F(p)$, where $F(p)$ is the distribution of all accelerated particles injected in the interstellar medium over SNR lifetime. (The total number of accelerated particles is $\int Q(p) dp$). It was assumed that the acceleration ceased at $t_c = 10^5$ yr. The shock velocity at this moment is close to 200 km/s and the maximum energy of protons confined in the supernova remnant is ~ 10 TeV. All particles with higher energies accelerated earlier have left the remnant. The maximum particle energy at late stages of shock evolution can be much smaller if one takes into account the possible damping of turbulence in the shock precursor due to ion-neutral collisions or non-linear wave interactions [11].

The function $F(p)$ was calculated as the sum of two integrals: the integral taken at t_c over the volume of supernova remnant $(4\pi) \int_0^{R_{\text{sh}}(t_c)} f(t_c, r, p) r^2 dr$, and the integral over time of the diffusion flux of accelerated particles through the boundary of the calculation domain $[4\pi r^2 \int_0^{t_c} (-D \partial f / \partial r) dt]_{r_b}$. The source function $Q(p)$ should be multiplied by ν_{sn} , where ν_{sn} is the supernova rate per unit volume to obtain the density of cosmic ray sources. Fig. 1 shows that about 1/3 of supernova explosion kinetic energy E goes to cosmic rays, which is in agreement with the empirical model of cosmic ray origin.

The spectrum of accelerated energetic ions other than protons has the same shape if expressed as a function of magnetic rigidity $Q(p/Z)$ with the appropriate absolute normalization determined by the injection process at thermal energies.

Released into interstellar space from numerous supernova remnants, the relativistic ions diffuse in galactic magnetic fields, interact with interstellar gas, and finally escape through the cosmic ray halo boundaries into intergalactic space, where the density of cosmic rays is negligible. The main characteristics of cosmic ray propagation in the Galaxy needed for the calculation of the cosmic ray spectrum is the escape length X_e , the average matter thickness traversed by cosmic rays before exit from the Galaxy. Based on [14] we choose it in the form

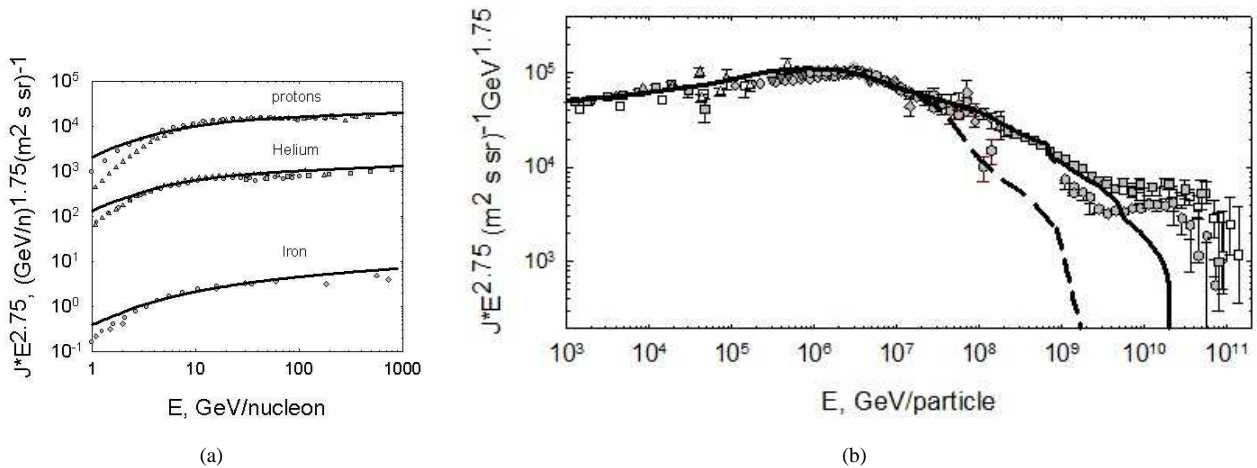


Fig. 2: (a) The calculated interstellar (not corrected for solar modulation at low energies) spectra of protons, Helium, and Iron below energy 10^3 GeV/n. (b) The all particle spectrum above 10^3 GeV; solid and dash lines are explained in the text. See [13] for references to the observational data shown by grey symbols.

$$X_e = \frac{11.8 (v/c)}{1 + (p/4.9ZGV)^{0.54}} g/cm^2. \quad (3)$$

Eq. (3) means that at high enough energies the resulting spectrum is steeper than the source spectrum by 0.54.

The results of our calculations are shown in Fig. 2a for the interstellar spectra of protons, Helium and Iron nuclei at kinetic energy per nucleon $1 \text{ GeV}/n < E < 10^3 \text{ GeV}/n$ where the charge resolution of cosmic ray experiments is high. The combined spectrum of all protons and ions with energies $E \geq 10^3 \text{ GeV}$ is shown by the solid line in Fig. 2b. The source calibration for nuclei from protons to Iron was made at one reference energy 10^3 GeV . It was assumed that the charge composition of accelerated particles was the same in all types of SNRs except that the highest energy part of the spectrum produced by Type Ib/c supernovae at $pc/Z > 3 \cdot 10^5 \text{ GeV}$ had no hydrogen that reflects the composition of highly evolved presupernovae.

The calculated spectra show remarkably good overall fit to observations up to ultra high energies $\sim 3 \cdot 10^9 \text{ GeV}$. To a good approximation the bending of the observed spectrum at around the knee energy $3 \cdot 10^6 \text{ GeV}$ is reproduced although no special efforts were made to force the theory fit the data. The bending is due to the combined effect of the summation over different types of SNRs and over different types of accelerated nuclei.

The complicated chemical composition of high energy cosmic rays is illustrated in Fig. 3 where the calculated mean logarithmic atomic number of cosmic rays $\langle \ln(A) \rangle$ is presented. The increase of $\langle \ln(A) \rangle$ at energies from 10^5 GeV to 10^7 GeV is due to the dependence of the knee position on charge $p_{\text{knee}} \propto Z$ for each kind of ions accelerated in Types Ia, IIP, Ib/c SNRs. Type IIB SNRs with normal composition dominate at rigidities $p/Z > 5 \cdot 10^6 \text{ GV}$. They have a knee at about

$p_{\text{knee}}/Z \approx 5 \cdot 10^7 \text{ GV}$ and provide progressively heavier composition to the very high energies.

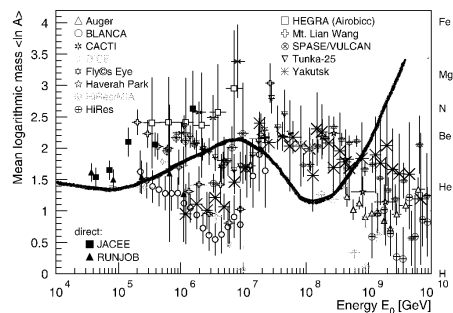


Fig. 3: Calculated mean logarithmic mass of cosmic rays (thick solid line) compared to observational data based on the average depth of shower maximum from [13].

The obtained cosmic ray spectrum shown by solid line in Fig. 2b is very attractive for the explanation of cosmic ray data. However, the use of the escape length (3) at ultra high energies is not justified. Experimentally, the value of X_e is determined from the abundance of secondary nuclei in cosmic rays with good statistics only up to about $100 \text{ GeV}/n$, see [14]. If cosmic ray transport in the Galaxy is described as diffusion, the diffusion coefficient can be expressed through the escape length as $D \approx v\mu H/2X_e$ (here $\mu \approx 0.003 \text{ g/cm}^2$ is the surface mass density of Galactic gas disk, $H \approx 4 \text{ kpc}$ is the height of the Galactic cosmic-ray halo), which gives $D \approx 1.3 \cdot 10^{28} (pc/Z \text{ GeV}) \text{ cm}^2/\text{s}$. The diffusion approximation can be applied when the diffusion mean free path $3D/v$ is less than the size of the system H , which results in the condition $pc/Z < 2 \cdot 10^7 \text{ GeV}$. The dash line in Fig. 2b shows the result of calculations made under the assumption that cosmic ray particles with energies $pc > 2 \cdot 10^7 Z \text{ GeV}$ are lost from the Galaxy

undetected. The predicted spectrum fits observations only up to $\sim 4 \cdot 10^7$ in this case.

The validity of diffusion approximation extends to higher energies in the diffusion model with distributed reacceleration on the interstellar turbulence where $X_e \propto (p/Z)^{1/3}$ at high rigidities, see [15]. However, this scaling does not reproduce the observed cosmic ray spectrum for the calculated source spectrum.

The physical pattern of cosmic ray propagation is different in the models with Galactic wind. The wind model with selfconsistently calculated cosmic-ray transport coefficients reproduces well the data on secondary nuclei [16]. The supersonic wind is probably terminated by the shock at ~ 0.5 Mpc from the Galactic disk. The confinement of very high energy cosmic rays in the Galaxy can be more efficient in this model as compared to the diffusion model with a static flat halo of the size ~ 4 kpc discussed above. In any case, trajectory calculations in galactic magnetic fields are needed to study cosmic ray propagation when the diffusion approximation breaks up at ultra high energies. The detailed consideration of this issue is beyond the scopes of the present paper.

III. CONCLUSION

We have calculated the steady state spectrum of cosmic rays produced by SNRs in the Galaxy. The new numerical code [5] for modelling of particle acceleration by spherical shocks with the back reaction of cosmic ray pressure on the shock structure was used in the calculations. The significant magnetic field amplification in young SNRs inferred from the observations of their synchrotron X-ray radiations [4], and most probably produced by cosmic ray streaming instability, was introduced in the calculations. It lead to the inclusion of the Alfvénic drift in the equation for particle transport downstream of the shock. Four different types of SNRs with relative burst rates taken from [10] were included in the calculations. The escape length Eq.(3) from [12] was used to describe the propagation of cosmic rays in the Galaxy. The normalization to the observed intensity and chemical composition of cosmic rays was made only at one energy, 10^3 GeV.

The results are illustrated by the solid line in Fig. 2b when Eq.(3) for X_e is used without limitation and by the dash line when it is limited by the applicability of the diffusion approximation for cosmic ray propagation in the diffusion model with a flat static halo. The solid line reproduces well the whole cosmic ray spectrum up to $\sim 3 \cdot 10^9$ GeV while the dash line makes it up to $\sim 4 \cdot 10^7$ GeV. Further investigations of cosmic rays propagation in galactic magnetic fields at ultra high energies are needed to refine the predicted shape of the spectrum produced by the Galactic SNRs. This is important in light of the discussion about transition from the Galactic to extragalactic component in the observed cosmic ray spectrum [17,18].

Our results can be compared to the earlier results [19] where the Alfvénic drift effect was not taken into account and only one type of SNRs (the Type Ia SNRs which represent about 30% of all SNRs) was considered. The absence of Alfvénic drift leads to the very flat cosmic ray source spectrum that required too strong dependence of the escape length on rigidity $X_e \propto (p/Z)^{-0.75}$, which is inconsistent with the available data on secondary nuclei.

Our assumption that the composition of accelerated particles is the same for all types of nuclei (except the very high energy part of the spectrum produced by Type Ia SNRs) and our ignoring of the dispersion of SNR parameters within the same type of supernovae are probably too simplified to correspond to reality. More comprehensive analysis with the account of earlier works [20], [21], [22] is needed, although that requires the introduction of new, not well known astrophysical parameters.

Another important problem is the discrete nature of supernovae in space and time leading to fluctuations that are difficult to account for. The number of supernovae that determines the cosmic ray intensity is ~ 20 at $10^8 Z$ GeV. The fluctuations of cosmic ray intensity and anisotropy in the diffusion model were studied in [23].

IV. ACKNOWLEDGMENTS

This work was supported by the RFBR grant 07-02-00028 at IZMIRAN and by the NASA APRA grant at IPST.

REFERENCES

- [1] F. Aharonian et al. 2007 A&A 464, 253; astro-ph/0611813v1
- [2] P.O. Lagage, C.J. Cesarsky. 1983 A&A 125, 249
- [3] A.R. Bell. 2004 MNRAS 353, 550
- [4] H.J. Völk, E.G. Berezhko, L.T. Ksenofontov. 2005 A&A 433, 229
- [5] V.N. Zirakashvili, V.S. Ptuskin. 2008 in *High-energy gamma-ray astronomy*, eds. F.A. Aharonian et al., Melville, NY, 2009, AIP Conf. Proc. 1085, p. 336
- [6] V.N. Zirakashvili. 2007 A&A 466, 1
- [7] V.N. Zirakashvili, V.S. Ptuskin. 2008 Ap. J. 678, 939
- [8] V.S. Ptuskin, V.N. Zirakashvili. 2005 A&A 429, 755
- [9] R. Chevalier. 2006 ApJ 651, 381
- [10] S.J. Smartt, J.J. Eldridge, R.M. Crockett, J.R. Maund. 2009 astro-ph/0809.0403v2
- [11] V.S. Ptuskin, V.N. Zirakashvili. 2003 A&A 403, 1
- [12] F.C. Jones et al. 2001 ApJ 547, 264
- [13] J. Bluemer, R. Engel, J.R. Hörandel. 2009, astro-ph/0904.0725v1
- [14] A.W. Strong, I.V. Moskalenko, V.S. Ptuskin. 2007 Annu. Rev. Nucl. Part. Sci. 57, 285
- [15] E.S. Seo, V.S. Ptuskin. 1994 ApJ 431, 705
- [16] V.S. Ptuskin, H.J. Völk, V.N. Zirakashvili, D. Breitschwerdt. 1997 A&A 321, 434
- [17] V.S. Berezhinsky. 2007 30th ICRC, Merida, highlight paper; astro-ph/0710.2750v2
- [18] A.M. Hillas. 2006 astro-ph/0607109v2
- [19] E.G. Berezhko, H.J. Völk. 2007 ApJ 661, L175
- [20] R. Silberberg, C.H. Tsao, M.M. Shapiro, P.L. Biermann. 1991, in *Cosmic Rays, Supernovae, Interstellar Medium*, eds. M.M.Shapiro, R. Silberberg, J.P. Wefel, Kluwer Ac. Publ., p. 97.
- [21] L.G. Sveshnikova. 2003 A&A 409, 799
- [22] A.S. Popescu. 2007 astro-ph/0704.2718v1
- [23] V.S. Ptuskin, F.C. Jones, E.S. Seo, R.S. Sina. 2006 Adv. Space Res. 37, 1909